1961 - april

NEW YORK UNIVERSITY

College of Engineering
RESEARCH DIVISION
University Heights, New York 53, N. Y.

Department of Meteorology and Oceanography

MODELS OF RANDOM SEAS BASED ON THE LAGRANGIAN EQUATIONS OF MOTION

by

Willard J. Pierson, Jr.

Technical Report Prepared for
the Office of Naval Research
under contract
Nonr-285(03)

NEW YORK UNIVERSITY
COLLEGE OF ENGINEERING
RESEARCH DIVISION

Department of Meteorology and Oceanography

Models of Random Seas Based on the Lagrangian Equations of Motion

by
Willard J. Pierson, Jr.

Technical Report Prepared for
the Office of Naval Research
under contract
Nonr-285(03)

April 1961

Models of Random Seas Based on the
Lagrangian Equations of Motion

ERRATA

Page 10,	eqn (25)	for z_{2t} read z_{2tt}
Page 20,	eqn (38)	second integral, read $\exp(-t^2/2)$
Page 21,	eqn (43)	for k read K
	eqn (47)	$E(z^3) = -3\psi_1\psi_o$
	eqn (48)	for ψ_2 read ψ_o
Page 22,	eqn (53)	$E(z')^3 = -2\psi_1^3$
	line 1	The skewness is not zero, and

Introduction

The present state of theoretical knowledge of wind generated gravity waves, when studied as a random process in nature, is based on a short crested Gaussian sea surface obtained by linearizing the Eulerian equations of motion (Pierson [1952], [1955]; Longuet-Higgins [1957]), on a second order extension of the Eulerian equations for long crested waves in which the underlying linear waves are Gaussian (Tick [1959]), and on various results involving wave spectra that do not specify the probability structure of the waves, some of which involve nonlinear properties of the waves (Phillips [1958], [1961]).

The short crested Gaussian model has proved fairly useful in explaining the angular spreading and dispersion of swell, the marked variation in height from wave to wave in a storm sea, wave refraction, bottom pressure fluctuations caused by waves passing overhead, and the motions of ships in waves (St. Denis and Pierson [1953], Lewis [1955], Cartwright and Rydill [1956]).

These applications are dependent on either the gross features of the waves or on natural processes that appear to linearize the system even further. For example, the wave profiles are in a sense averaged over the length and beam of a vessel at sea, and the nonlinear effects are reduced. The higher harmonics in a nonlinear profile and the high frequency linear components are also attenuated with depth in such a way that the application of Gaussian noise theory to the zero crossings of bottom pressure fluctuations leads to useful results (Ehrenfeld, Goodman, et al [1958]).

The spectrum of the time process at a fixed point has been most frequently studied. Since the actual wave is recorded, more or less, the full nonlinear motion is recorded, and the spectrum of this nonlinear motion is estimated. The accuracy of computations in a linear theory based on spectra estimated from a nonlinear record is open to question. In particular, higher moments of the spectra are quite open to question.

Theoretical developments in the study of the short crested Gaussian sea surface require numerous higher moments of the linear part

of the process. If computed spectra are used to estimate these moments, many of the higher moments are obscured by high frequency white noise in the estimate or made questionable by the high frequency nonlinear part of the spectrum so that the results predicted from them are doubtful. If the various theoretical forms for the spectra that have been proposed are used, the fourth or fifth moment of the frequency spectrum becomes questionable and the meaning of the second or third moment in the wave number spectrum is obscure.

These problems are further complicated by the fact that sea surface slopes depend on the very high frequency capillary waves. With capillary waves, breakers, whitecaps and turbulence in the upper layers of the water, any results on curvature, as they depend on the higher moments of the spectrum, are highly doubtful for a storm sea.

The actual sea surface has gross features that are not in accord with the short crested Gaussian model. No artist, for example, depicts wind waves as irregular sinusoidal waves. Wave profiles along a line as a function of distance show sharp crests and long shallow troughs that do not occur in the model. This point will be discussed further in a later part of this paper.

Purpose of paper

The purpose of this paper is to derive three new random seaway models that appear to have some properties of actual seas not illustrated by previous models, to derive a few of these properties and discuss other possible properties, and to show how these models appear to be more realistic by comparing them with selected observations. These new models explain some of the difficulties that arise with the higher spectral moments. They may also be capable of giving some information about whitecaps, breaking waves, and sharp crested waves. Since all mathematical models of nature fail in one way or the other when the conditions and assumptions in the derivation are not met, these models will provide a second choice when observations of waves are to be compared with theoretical results. Some questions are raised that can only be answered by additional theoretical work and by precise measurements of waves. The theoretical properties of these models can be compared with the theoretical

properties of those models described above in order to design more definitive experiments concerning the nature of wind generated waves.

The Lagrangian equations

Let α, β, and δ be the x, y, and z coordinates of a particle of fluid. In the Lagrangian system of equations, a solution to the equations consists of finding the positions x, y, and z of all of the particles in the fluid as a function of time and the initial positions of the particles, α, β, and δ. The Lagrangian equations, according to Lamb [1932] are given by equations (1) where subscripts denote partial differentiation.

$$\begin{aligned} &x_{tt}x_\alpha + y_{tt}y_\alpha + (z_{tt}+g)z_\alpha + p_\alpha/\rho = 0 \\ (1)\qquad &x_{tt}x_\beta + y_{tt}y_\beta + (z_{tt}+g)z_\beta + p_\beta/\rho = 0 \\ &x_{tt}x_\delta + y_{tt}y_\delta + (z_{tt}+g)z_\delta + p_\delta/\rho = 0 \end{aligned}$$

The equation of continuity is most conveniently expressed by

$$(2)\qquad \frac{d}{dt}\left[\frac{\partial(x,y,z)}{\partial(\alpha,\beta,\delta)}\right] = 0$$

Such solutions need not be irrotational, but, if a function, $F(\alpha,\beta,\delta,t)$, can be found such that

$$(3)\quad dF = (x_t x_\alpha + y_t y_\alpha + z_t z_\alpha)d\alpha + (x_t x_\beta + y_t y_\beta + z_t z_\beta)d\beta + (x_t x_\delta + y_t y_\delta + (z_t z_\delta)d\delta$$

is a perfect differential, there is no vorticity.

A zero order solution to these equations is given by

$$\begin{aligned} x &= \alpha \\ y &= \beta \\ (4)\qquad z &= \delta \\ p &= p_o - g\rho\delta \end{aligned}$$

in which all fluid particles are at rest in hydrostatic equilibrium under the force of gravity.

We expand, following the concepts described by Stoker [1957], about the zero order solution in terms of a small parameter, ε , as in (5) in which F_o is a constant. Here we think of ε as equal to ak ,

but the first order terms must have the dimensions of a length, and so $a = \varepsilon/k$ is used in the various solutions that are obtained. The parameter ε never appears explicitly. See, for example, Longuet-Higgins [1953], and Pierson and Fife [1961] for different ways that ε can be interpreted.

$$\begin{aligned}
x &= \alpha + \varepsilon x_1 + \varepsilon^2 x_2 \\
y &= \beta + \varepsilon y_1 + \varepsilon^2 y_2 \\
z &= \delta + \varepsilon z_1 + \varepsilon^2 z_2 \\
p &= p_o - g\rho\delta + \varepsilon p_1 + \varepsilon^2 p_2 \\
F &= F_o + \varepsilon F_1 + \varepsilon^2 F_2
\end{aligned} \tag{5}$$

The equations in ε become

$$\begin{aligned}
& x_{1tt} + g z_{1\alpha} + p_{1\alpha}/\rho = 0 \\
& y_{1tt} + g z_{1\beta} + p_{1\beta}/\rho = 0 \\
& z_{1tt} + g z_{1\delta} + p_{1\delta}/\rho = 0 \\
& x_{1\alpha t} + y_{1\beta t} + z_{1\delta t} = 0 \\
& dF_1 = x_{1t}\, d\alpha + y_{1t}\, d\beta + z_{1t}\, d\delta
\end{aligned} \tag{6}$$

The equations in ε^2 become

$$\begin{aligned}
& x_{2tt} + g z_{2\alpha} + p_{2\alpha}/\rho = - x_{1tt} x_{1\alpha} - y_{1tt} y_{1\alpha} - z_{1tt} z_{1\alpha} \\
& y_{2tt} + g z_{2\beta} + p_{2\beta}/\rho = - x_{1tt} x_{1\beta} - y_{1tt} y_{1\beta} - z_{1tt} z_{1\beta} \\
& z_{2tt} + g z_{2\delta} + p_{2\delta}/\rho = - x_{1tt} x_{1\delta} - y_{1tt} y_{1\delta} - z_{1tt} z_{1\delta} \\
& [x_{2\alpha} + y_{2\beta} + z_{2\delta} + y_{1\beta} x_{1\alpha} + x_{1\alpha} z_{1\delta} + y_{1\beta} z_{1\delta} - z_{1\alpha} y_{1\delta} \\
& \qquad - z_{1\beta} y_{1\alpha} - x_{1\beta} y_{1\alpha}]_t = 0 \\
& dF_2 = (x_{2t} + x_{1t} x_{1\alpha} + y_{1t} y_{1\alpha} + z_{1t} z_{1\alpha}) d\alpha + (y_{2t} + x_{1t} x_{1\beta} + y_{1t} y_{1\beta} + z_{1t} z_{1\delta}) d\beta \\
& \qquad + (z_{2t} + z_{1t} y_{1\delta} + y_{1t} y_{1\delta} + z_{1t} z_{1\delta}) d\delta
\end{aligned} \tag{7}$$

Equations (6) are linear. A solution of them in turn determines the right hand side of (7). Since the left hand side of (7) is linear, in principle at least, a solution can be found. Also in principle (though not in practice), it is possible to proceed to as high an order as desired by this procedure.

The Gerstner wave

A solution to equations (6), applicable to waves in deep water, when added to the zero order solution, yields equation (8).

$$x = \alpha + \varepsilon x_1 = \alpha - \frac{ak_1}{k} e^{k\delta} \sin(k_1\alpha + k_2\beta - \omega t)$$

$$y = \beta + \varepsilon y_1 = \beta - \frac{ak_2}{k} e^{k\delta} \sin(k_1\alpha + k_2\beta - \omega t)$$

(8) $$z = \delta + \varepsilon z_1 = \delta + a\, e^{k\delta} \cos(k_1\alpha - k_2\beta - \omega t)$$

$$p = p_o + \varepsilon p_1 = p_o - g\rho\delta$$

$$F_1 = \frac{a\omega}{k} e^{k\delta} \sin(k_1\alpha + k_2\beta - \omega t)$$

In order to impose the condition that $p(\alpha, \beta, \delta) = p_o$ at $\delta = 0$, it is required that

(9) $$\frac{\omega^2}{g} = k$$

The continuity equation imposes the condition that

(10) $$k^2 = k_1^2 + k_2^2$$

The first order solution has no vorticity to first order as F_1 has been found.

An alternate form for the solution given by (8) is (11).

$$x = \alpha - a \cos\theta\, e^{\omega^2\delta/g} \sin(\frac{\omega^2}{g} (\alpha \cos\theta + \beta \sin\theta) - \omega t)$$

(11) $$y = \beta - a \sin\theta\, e^{\omega^2\delta/g} \sin(\frac{\omega^2}{g} (\alpha \cos\theta + \beta \sin\theta) - \omega t)$$

$$z = \delta + a\, e^{\omega^2\delta/g} \cos(\frac{\omega^2}{g} (\alpha \cos\theta + \beta \sin\theta) - \omega t)$$

These solutions (eqs. 8 and 11) are simply disguised versions of the Gerstner wave in deep water as described in Lamb. The angle θ is the direction toward which the wave is traveling. When the solution is periodic, as above, the original nonlinear equations are satisfied exactly, but it can be shown that there is some second order vorticity and that there is a second order correction to the pressure given by

$$p = p_o - g\rho\delta + \frac{a^2 k}{2} g\rho e^{2k\delta} - \frac{a^2 k}{2} g\rho \tag{12}$$

Another possibility also suggests itself. With $x_2 = a^2 \omega k t e^{2k\delta} \cos\theta$, $y_2 = a^2 \omega k t e^{2k\delta} \sin\theta$, and $z_2 = 0$, equations (1), (2), and (3) are still satisfied to second order but third order complications arise. These two terms are the equivalent of the second order current found in irrotational waves in the Eulerian system of equations as described in Lamb.

Extension of these results to finite depth would probably follow the results of Biesel [1952] who achieved a remarkable representation for periodic breaking waves by means of the Lagrangian equations (see also Pierson [1955]).*

A randomized short crested model

The expressions for x_1, y_1, and z_1 in either (8) or (11) are solutions of equations (6). These equations are linear. Therefore, a sum, over different parameter values, of solutions of the form of x_1, y_1, and z_1 will also be a solution. If it is assumed that each particle has a displacement from its rest position, $\alpha_o, \beta_o, \delta_o$, that is described by a stationary Gaussian vector process with specified coherency relationships, a solution to equations (1) that is correct to first order is given by equations (13).

$$\begin{aligned}
x &= \alpha - \int_0^\infty \int_{-\pi}^{\pi} e^{\omega^2 \delta/g} \cos\theta \sin\left(\frac{\omega^2}{g}(\alpha\cos\theta + \beta\sin\theta(-\omega t + \epsilon(\omega,\theta)\right)\right) \sqrt{2S(\omega,\theta)\, d\theta\, d\omega} \\
y &= \beta - \int_0^\infty \int_{-\pi}^{\pi} e^{\omega^2 \delta/g} \sin\theta \sin\left(\frac{\omega^2}{g}(\alpha\cos\theta + \beta\sin\theta) - \omega t + \epsilon(\omega,\theta)\right) \sqrt{2S(\omega,\theta)\, d\theta\, d\omega} \\
z &= \delta + \int_0^\infty \int_{-\pi}^{\pi} e^{\omega^2 \delta/g} \cos\left(\frac{\omega^2}{g}(\alpha\cos\theta + \beta\sin\theta) - \omega t + \epsilon(\omega,\theta)\right) \sqrt{2S(\omega,\theta)\, d\theta\, d\omega}
\end{aligned} \tag{13}$$

---

*The remarks concerning the Gerstner wave are in error as these results six years later show.

The notation here is that used by Pierson (1952, 1955) except $S(\omega, \theta)$ is the resolution of the variance of the particle motions into frequency and direction. For some fixed particle, say, one at the surface given by $\alpha = 0$, $\beta = 0$, $\delta = 0$, the motions $x = x(t)$, $y = y(t)$, and $z = z(t)$ form a stationary vector Gaussian process such that the spectrum of $x(t)$ is

$$\int S(\omega, \theta)(\cos\theta)^2 d\theta \text{ ,}$$

the spectrum of $y(t)$ is

$$\int S(\omega, \theta)(\sin\theta)^2 d\theta \text{ ,}$$

the spectrum of $z(t)$ is

$$\int S(\omega, \theta)\, d\theta \text{ ,}$$

the cospectrum of $x(t)\,y(t)$ is

$$\int S(\omega, \theta) \cos\theta \sin\theta \, d\theta \text{ ,}$$

the quadrature spectrum of $x(t)\,z(t)$ is

$$\int S(\omega, \theta) \cos\theta \, d\theta \text{ ,}$$

the quadrature spectrum of $y(t)\,z(t)$ is

$$\int S(\omega, \theta) \sin\theta \, d\theta \text{ ,}$$

and all other cross spectra are zero.

Other notations are often useful. For example, a notation similar to that of Longuet-Higgins [1957] would yield (14) as the complete equivalent of (13).

$$\begin{aligned} x &= \alpha - \Sigma a_{mn} \frac{k_m}{k_{mn}} e^{k\delta} \sin(k_m \alpha + k_n \beta - \omega_{mn} t + \epsilon_{mn}) \\ y &= \beta - \Sigma a_{mn} \frac{k_n}{k_{mn}} e^{k\delta} \sin(k_m \alpha + k_n \beta - \omega_{mn} t + \epsilon_{mn}) \qquad (14) \\ z &= \delta + \Sigma a_{mn} e^{k\delta} \cos(k_m \alpha + k_n \omega - \omega_{mn} t + \epsilon_{mn}) \end{aligned}$$

In (14), added conditions are that

$$k_m^{\ 2} + k_n^{\ 2} = k_{mn}^2 \qquad (15)$$

and that

(16) $$\frac{\omega_{mn}^2}{g} = \sqrt{k_m^2 + k_n^2}$$

The free surface

Those particles on the free surface are described by the condition $\delta = 0$ and (13) becomes

$$x = x(\alpha,\beta,t) = \alpha - \int_0^\infty \int_{-\pi}^{\pi} \sin(\frac{\omega^2}{g}(\alpha\cos\theta + \beta\sin\theta) - \omega t + \epsilon)\cos\theta\ \sqrt{2S(\omega,\theta)\,d\theta\,d\omega}$$

(17) $$y = y(\alpha,\beta,t) = \beta - \int_0^\infty \int_{-\pi}^{\pi} \sin(\frac{\omega^2}{g}(\alpha\cos\theta + \beta\sin\theta) - \omega t + \epsilon)\sin\theta\ \sqrt{2S(\omega,\theta)\,d\theta\,d\omega}$$

$$z = z(\alpha,\beta,t) = \int_0^\infty \int_{-\pi}^{\pi} \cos(\frac{\omega^2}{g}(\alpha\cos\theta + \beta\sin\theta) - \omega t + \epsilon)\sqrt{2S(\omega,\theta)\,d\theta\,d\omega}$$

In principle, and perhaps admitting triple values for the inverses over limited regions in the x, y, t space, $x = x(\alpha,\beta,t)$ and $y = y(\alpha,\beta,t)$ imply inverses of the form

(18) $$\alpha = \alpha(x,y,t) \quad \text{and} \quad \beta = \beta(x,y,t)$$

so that the free surface can be found from

(19) $$z = z(\alpha(x,y,t),\ \beta(x,y,t)t) = z(x,y,t)\ .$$

The surface so defined is certainly not the equivalent of the short crested Gaussian sea surface. The short crested Gaussian sea surface is equivalent to this representation when the amplitude of the particle motions becomes so small that $\alpha = x$ and $\beta = y$ are satisfactory approximations to the inverses given by (18). Otherwise, further study suggests that $z = z(x,y,t)$ has many features of actual waves in that the crests can be quite sharply pointed and in that the higher nonlinear harmonics that occur in the higher order derivations in the Eulerian system are already present in this model.

It is believed that the problems that arise in the adequate probabilistic description of the surface defined by (19) in terms of (17) and (18) will be very difficult to solve and that considerable effort will be required. All of the problems that arise in the study of Gaussian noise and in the study of the short crested Gaussian sea surface have their analogue in this

model.

Second order effects in the short crested model

For reasons to be discussed later, it may be necessary to proceed to second order in this model and determine the effects of equations (7) on the wavy surface especially if breaking waves are to be studied.

The long crested linear model

If $S(\omega, \theta)$ becomes concentrated at the angle $\theta = 0$ and degenerates to a function of ω only, equations (13) become

$$x = x(\alpha, \delta, t) = \alpha - \int_0^\infty e^{\omega^2 \delta/g} \sin(\frac{\omega^2}{g} \alpha - \omega t + \epsilon) \sqrt{2S(\omega)\, d\omega}$$

$$y = y(\beta) = \beta \tag{20}$$

$$z = z(\alpha, \delta, t) = \delta + \int_0^\infty e^{\omega^2 \delta/g} \cos(\frac{\omega^2}{g} \alpha - \omega t + \epsilon) \sqrt{2S(\omega)\, d\omega}$$

An alternate notation is given by

$$x = \alpha - \Sigma\, a_n\, e^{k_n \delta} \sin(k_n \alpha - \omega_n t + \epsilon_n)$$

$$z = \delta - \Sigma\, a_n\, e^{k_n \delta} \cos(k_n \alpha - \omega_n t + \epsilon_n) \tag{21}$$

For δ equal to zero, the inverse of the first equation is

$$\alpha = \alpha(x, t) \tag{22}$$

This implies a free surface given by

$$z = z(\alpha(x, t), t) = z(x, t) \tag{23}$$

Second order effects in the long crested model

The long crested model is more amenable to an investigation of second order effects because it is simpler. We consider the problem of two waves, and then generalize to the randomized process. For two waves the linear solution is given by

$$
\begin{aligned}
& x_1 = -a_1 e^{k_1\delta} \sin(k_1 a - \omega_1 a + \epsilon_1) - a_2 e^{k_2\delta} \sin(k_2 a - \omega_2 t + \epsilon_2) \\
(24)\quad & z_1 = a_1 e^{k_1\delta} \cos(k_1 a - \omega_1 t + \epsilon_1) + a_2 e^{k_2\delta} \cos(k_2 a - \omega_2 t + \epsilon_2) \\
& p_1 = 0 \\
& F_1 = \frac{a_1\omega_1}{k_1} e^{k_1\delta} \sin(k_1 a - \omega_1 t + \epsilon_1) + \frac{a_2\omega_2}{k_2} e^{k_2\delta} \sin(k_2 a - \omega_2 t + t_2)
\end{aligned}
$$

It is irrotational to first order. For simplicity, we assume that $\omega_2 > \omega_1$.

The second order equations to be solved are obtained by substituting (24) into (7) where y is set equal to β only and all partials with respect to β vanish. These equations are given by

$$x_{2tt} + g z_{2a} + p_{2a}/\rho = 0$$

$$z_{2t} + g z_{2\delta} + p_{2\delta}/\rho = g(a_1^2 k_1^2 e^{2k_1\delta} + a_2^2 k_2^2 e^{2k_2\delta}$$

$$+ 2a_1 a_2 k_1 k_2 e^{(k_1+k_2)\delta} \cos((k_2 - k_1)a - (\omega_2 - \omega_1)t + \epsilon_2 - \epsilon_1))$$

$$[25]\quad [x_{2a} + z_{2\delta} - 2a_1 a_2 e^{(k_1+k_2)\delta} \cos((k_2 - k_1)a - (\omega_2 - \omega_1)t + \epsilon_2 - \epsilon_1)]_t = 0$$

$$dF_2 = [x_{2t} - (a_1^2 k_1 \omega_1 e^{2k_1\omega_1} e^{2k_1\delta} + a_2^2 k_2 \omega_2 e^{2k_2\delta}$$

$$+ a_1 a_2(\omega_1 k_2 + \omega_2 k_1) e^{(k_1+k_2)\delta} \cos((k_2 - k_1)a - (\omega_2 - \omega_1)t + \epsilon_2 - \epsilon_1))]da$$

$$+ [(z_{2t} - (\frac{a_1 a_2}{g}(\omega_2 - \omega_1)(\omega_2\omega_1) e^{(k_1+k_2)\delta} \sin((k_2 - k_1)a - (\omega_2 - \omega_1)t + \epsilon_2 - \epsilon_1)]d\delta$$

In (25), we have four equations in p, z and x. The first three determine a solution, subject to appropriate boundary conditions, for p, z, and x. The last is then used to see if the solution is irrotational and to make the solution irrotational if possible. Note that $x = x_2(\delta)t$ can be added to (23), if desired, as part of the total solution to the equations. The boundary conditions are that $p_2 = 0$ at $\delta = 0$ and that x_2 and z_2 approach zero as δ approaches $-\infty$.

If the right hand side of the second equation is represented by $g[F(\delta) + G(a, \delta, t)]$ and the third equation is written as $x_{2a} + z_{2\delta} - G(a, \delta, t) = 0$,

it is possible by cross differentiating the first two equations, subtracting and combining the result with the third equation to obtain the result that

(26) $$z_{2tt\alpha\alpha} + z_{2tt\delta\delta} = G_{tt\delta} + g\,G_{\delta\delta}$$

This provides the inhomogeneous solution for $z_2(\alpha, \delta, t)$. The third equation then determines $x_2(\alpha, \delta, t)$ and the first two yield the same solution for p_2.

However p_2 does not satisfy the free surface condition, and a solution to the homogeneous equations must then be found that when added to this solution yields a proper form for p_2.

This provides solutions to the first three equations. When x_2 and z_2 are substituted into the last equation, it is seen that the vorticity can be made zero by adding $a_1^2 k_1 \omega_1 e^{2k_1\delta} t + a_2^2 k_2 \omega_2 e^{2k_2\delta} t$ to x_2.

The second order terms therefore become

$$x_2 = -\frac{a_1 a_2}{g}\left(\frac{\omega_1^3 + \omega_2^3}{\omega_2 - \omega_1}\right) e^{(k_2+k_1)\delta} \sin((k_2 - k_1)\alpha - (\omega_2 - \omega_1)t + \epsilon_2 - \epsilon_1)$$

$$+ \frac{a_1 a_2}{g}(\omega_2 + \omega_1)\omega_2\, e^{(k_2-k_1)\delta} \sin((k_2 - k_1)\alpha - (\omega_2 - \omega_1)t + \epsilon_2 - \epsilon_1)$$

$$+ a_1^2 \omega_1 k_1\, e^{2k_1\delta} t + a_2^2 \omega_2 k_2\, e^{2k_2\delta} t$$

(27) $$z_2 = \frac{a_1 a_2}{g}(\omega_1^2 + \omega_1\omega_2 + \omega_2^2) e^{(k_1+k_2)\delta} \cos((k_2 - k_1)\alpha - (\omega_2 - \omega_1)t + \epsilon_2 - \epsilon_1)$$

$$- \frac{a_1 a_2}{g}\omega_2(\omega_2 + \omega_1)\, e^{(k_2-k_1)\delta} \cos((k_2 - k_1)\alpha - (\omega_2 - \omega_1)t + \epsilon_2 - \epsilon_1)$$

$$p_2 = g\rho\frac{a_1^2 k_1}{2}(e^{2k_1\delta} - 1) + g\rho\frac{a_2^2 k_2}{2}(e^{2k_2\delta} - 1)$$

$$- 2\rho a_1 a_2 \omega_2 \omega_1\, e^{(k_1+k_2)\delta} \cos((k_2 - k_1)\alpha - (\omega_2 - \omega_1)t + \epsilon_2 - \epsilon_1)$$

$$+ 2\rho a_1 a_2 \omega_2 \omega_1\, e^{(k_2-k_1)\delta} \cos((k_2 - k_1)\alpha - (\omega_2\omega_1)t + \epsilon_2 - \epsilon_1)$$

$$F_2 = a_1 a_2 \omega_2\, e^{(k_2-k_1)} \sin((k_2 - k_1)\alpha - (\omega_2 - \omega_1)t + \epsilon_2 - \epsilon_1)$$

$$+ a_2 a_1(\omega_2 - \omega_1)\, e^{(k_2+k_1)} \sin((k_2 - k_1)\alpha - (\omega_2 - \omega_1)t + \epsilon_2 - \epsilon_1)$$

The full solution is obtained by combining equations (5), (24), and (27). This solution satisfies the equations to second order. It is irrotational to second order.

If more terms are added to the linear solution subject to the condition that $\omega_1 < \omega_2 < \omega_3 < \cdots < \omega_n$, the terms in the linear solution interact in a predictable way to generate appropriate second order terms. The randomized second order solution for $x(\alpha, \delta, t)$ and $z(\alpha, \delta, t)$ are given by equations (28).

$$\begin{aligned}
x(\alpha,\delta,t) = \alpha &- \Sigma a_i e^{k_i\delta} \sin(k_i\alpha - \omega_i t + \epsilon_i) \\
&- \sum_{j>i}\sum_{i} \frac{a_i a_j}{g}\left(\frac{\omega_i^3+\omega_j^3}{\omega_j-\omega_i}\right) e^{(k_j+k_i)\delta} \sin((k_j-k_i)\alpha-(\omega_j-\omega_i)t+\epsilon_j-\epsilon_i) \\
&+ \sum_{j>i}\sum_{i} \frac{a_i a_j}{g}(\omega_j+\omega_i)\omega_j e^{(k_j-k_i)\delta} \sin((k_j-k_i)\alpha-(\omega_j-\omega_i)t+\epsilon_j-\epsilon_i) \\
&+ \Sigma a_i^2 \omega_i k_i e^{2k_i\delta} t \\
z(\alpha,\delta,t) = \delta &+ \Sigma a_i e^{k_i\delta} \cos(k_i\alpha - \omega_i t + \epsilon_i) \\
&+ \sum_{j>i}\sum_{i} \frac{a_i a_j}{g}(\omega_i^2+\omega_i\omega_j+\omega_j^2) e^{(k_i+k_j)} \cos((k_j-k_i)\alpha-(\omega_j-\omega_i)t+\epsilon_j-\epsilon_i) \\
&- \sum_{j>i}\sum_{i} \frac{a_i a_j}{g}\omega_j(\omega_j+\omega_i) e^{(k_j-k_i)\delta} \cos((k_j-k_i)\alpha-(\omega_j-\omega_i)t+\epsilon_j-\epsilon_i)
\end{aligned} \tag{28}$$

The solution given by equation (28) has features that are quite different from solutions obtained by the assumption of irrotationality in the Eulerian system. The trigonometric second order terms involve only the difference between two frequencies. One of the second order terms dies out rapidly with depth. The other dies out slowly with depth. The term that is linear in t is the average drift of the particle, and as a group of higher waves passes, the effect of the second order terms is to increase the drift. Correspondingly, as low waves pass, the drift is decreased.

The positions of those particles that are on the free surface are obtained by setting $\delta = 0$, and the result is equation (29).

$$
\begin{aligned}
x(\alpha,t) &= \alpha - \Sigma a_i \sin(k_i\alpha - \omega_i t + \epsilon_i) \\
&\quad - \sum_{j>i} \sum_i \frac{a_i a_j}{g} \frac{\omega_i(\omega_j + \omega_i)}{\omega_j - \omega_i} \sin((k_j - k_i)\alpha - (\omega_j - \omega_i)t + \epsilon_j - \epsilon_i) + \Sigma a_i^2 \omega_i k_i t \\
z(\alpha,t) &= \Sigma a_i \cos(k_i\alpha - \omega_i t + \epsilon_i) \\
&\quad + \sum_{j>i} \sum_i \frac{a_i a_j}{g} \omega_i^2 \cos((k_j - k_i)\alpha - (\omega_j - \omega_i)t + \epsilon_j - \epsilon_i)
\end{aligned}
\tag{29}
$$

The parametric equations, $x = x(\alpha, t)$ and $z = z(\alpha, t)$, imply an inverse for $x = x(\alpha, t)$ such that $\alpha = \alpha(x, t)$, and so

$$z = z(\alpha(x, t), t) \tag{30}$$

is the equation for the free surface correct to second order as obtained by this solution of the Lagrangian equations of motion.

Comparison of the Lagrangian and Eulerian models

Results obtained in the Lagrangian system of equations are difficult to compare with results obtained in the Eulerian system of equations. In the Eulerian system the fluid velocity at a fixed point below the surface will be Gaussian in the linear Gaussian model. The velocity at a fixed point in the linear Gaussian model in the Lagrangian system has not been found but it involves finding

$$
\begin{aligned}
u &= \frac{dx}{dt} = u(\alpha(x, z, t),\ \delta(x, z, t),\ t)\ , \\
\alpha &= \alpha(x, z, t)\ , \quad \text{and} \\
\delta &= \delta(x, z, t)
\end{aligned}
\tag{31}
$$

from equations (21), even in the long crested case, and this velocity is not Gaussian unless the waves are so low that $\alpha = x$ and $\delta = z$ are sufficiently accurate inverses of $x = x(\alpha, \delta, t)$ and $z = z(\alpha, \delta, t)$.

However, a higher order model in the Eulerian system of equations may well yield velocities comparable to those given by a model to a lower order in the Lagrangian equations.

The first and second order models in the Lagrangian equations appear to have advantages over the comparable first and second order models in the Eulerian equations, as will be shown later. Since the

resulting free surface is non-Gaussian it may be just as difficult to obtain results on the probability structure of the first and second order Lagrangian models as it would be to obtain results on a much higher order Eulerian model. If the problems prove intractable, numerical computation is a possibility that should yield some results.

The real problem is thus to compare the six available random models with nature and to devise relevant experiments to see which model comes the closest to agreeing with that which is observed. Any linear non-Gaussian model that can be devised along with its higher order extensions should also be allowed to enter the competition. We suspect that such models will not do as well.

Recapitulation

So far in this paper, three new random sea surfaces have been obtained. They are the short crested sea surface given by (17), (18), and (19) based on a linear superposition of the particle motions; the long crested sea surface given by (21), (22), and (23) based on a linear superposition of the particle motions; and the long crested sea surface given by (29) and (30) based on the second order correction to the long crested model. Each model is irrotational to the order to which it is carried out. The notation chosen to represent the second order long crested model is not as useful as the notation used by Tick [1959] in his study of the second order long crested model in the Eulerian system. These results, however, show the existence of such a model.

Properties of the models

The multivariate probability structures of these models have not yet been found. Only a few of the properties of the long crested linear model have been found. A possible realization of $z = z(x)$ has been constructed, and the probability density of $z(x)$ for a fixed x has been found.

Construction of $z = z(x)$ for the linear model

With δ and t equal to zero in (21), the result is

$$
\begin{aligned}
x &= \alpha + x_1 = \alpha - \Sigma a_n \sin(k_n\alpha + \epsilon_n) \\
z &= z_1 = \Sigma a_n \cos(k_n\alpha + \epsilon_n)
\end{aligned}
\tag{32}
$$

The quantities x_1 and z_1 form a vector Gaussian process.* The spectrum of x_1 is S(k), the spectrum of z_1 is S(k), the co-spectrum is zero, and the quadrature spectrum is -S(k). The coherency is one.

Tick [1961] has developed procedures for the construction of vector Gaussian processes with required spectra, cross spectra, and coherencies. A vector process with a reasonable spectrum and with the proper cross spectra was available, and it was a simple matter to prepare graphs of $x(\alpha)$ and $z(\alpha)$ as a function of α.

The results are shown in figure 1, where $x_1(\alpha)$, $z(\alpha)$, and $\alpha + x_1(\alpha)$ are all graphed as a function of α. For any value of α in this figure, a pair of values for x and z result that can be plotted as a point in the x, z plane as shown immediately below. The points in the x, z plane then trace out the indicated curve that represents $z = z(x)$. Only two crests are shown in figure 1.

Figure 2 shows the result of preparing much longer graphs of $x(\alpha)$ and $z(\alpha)$. Eight crests are shown in the figure. In many ways, this artificial record appears to be much more realistic than one that might be obtained with a linear Gaussian model.

These results show that, although the spectrum of the orbital motion could be band limited (i. e., identically zero outside of a certain wave number range), the spectrum of $z = z(x)$ could be very rich in higher harmonics of the orbital motion spectrum. With one or more simple discontinuities in slope, as would be achieved at the sharp crests, the asymptotic form predicted by Phillips [1958] would be found as applied to the long crested case. However, it would occur at wave numbers much higher than are presently capable of being resolved in spectral analyses.

One of the difficulties with the Eulerian models is that they do not indicate within themselves unrealistic wave forms. A spectrum that would yield an impossible sea condition does not appear to be different from one that would yield a realistic sea condition. The linear Lagrangian model is

---

*In fact, z_1 is the Hilbert transform of x_1.

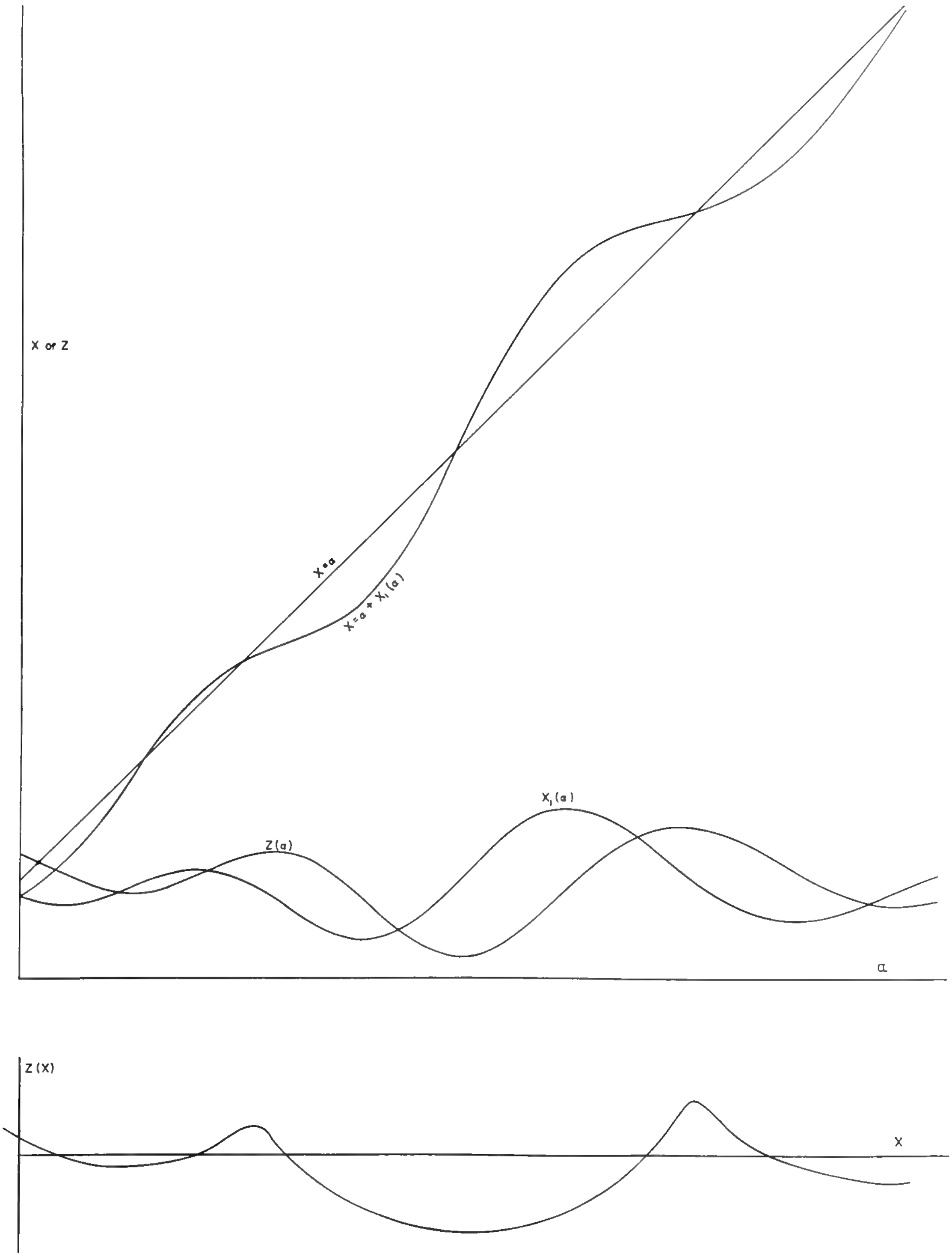

Fig. 1. GRAPHS OF $Z(\alpha)$, $X_1(\alpha)$, AND $X(\alpha)$ TO SHOW HOW $Z = Z(X)$ IS OBTAINED

Figure 2. PARAMETRIC SOLUTION OF $Z(\alpha)$ AND $X(\alpha)$ TO OBTAIN $Z = Z(X)$ AND WAVE PROFILES WITH SHARP CRESTS AND SHALLOW TROUGHS

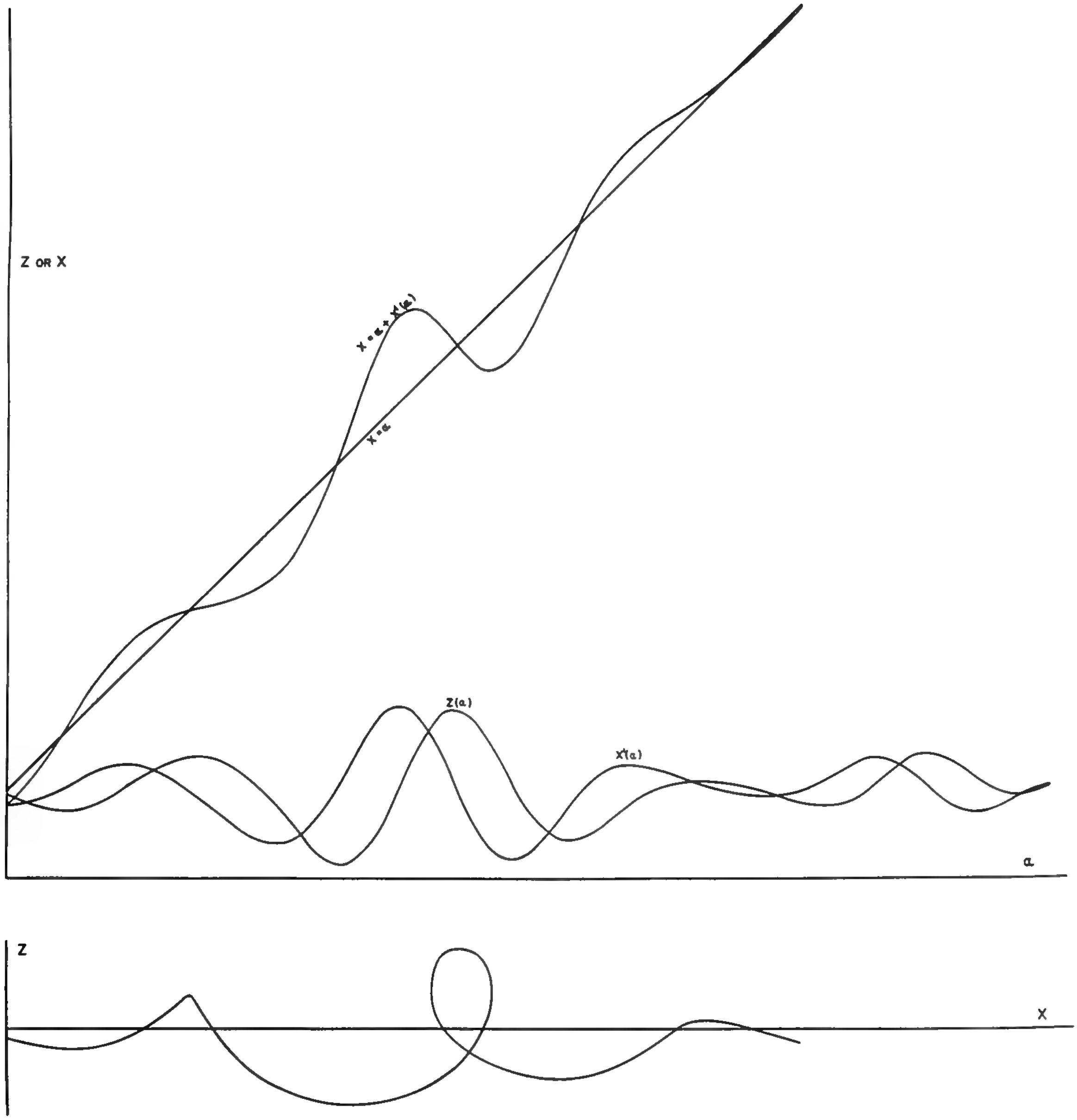

Figure 3. Parametric solution of $z(\alpha), x(\alpha)$ to obtain free surface $z = z(x)$ with loops.

already capable of differentiating between completely unrealistic spectra and more realistic ones. If the space scale of x_1 and z_1 is changed for the same vector realization used to construct figures 1 and 2, the result is figure 3. Here α is triple valued for a certain range of x, and when z(x) is plotted the surface forms a large loop. This may be indicative of a very unstable state in the waves that could not be attained in nature because breaking waves would form each time such a loop would be initiated in the space-time representation and the kinetic energy of the wave motion would be dissipated by turbulence in the whitecaps to an extent that the particle motion spectra would be modified to a more realistic condition.

Conditions for a loop in $z = z(x)$

A loop occurs in $z = z(x)$ if z is triple valued as a function of x. This in turn occurs if $x(\alpha)$ is not monotonically increasing. Thus if $m < 0$ where

$$m = \frac{dx}{d\alpha} = 1 - \Sigma a_n k_n \cos(k_n \alpha - \omega_n t + \epsilon_n) \tag{33}$$

a loop will form.

The probability that

$$\Sigma a_n k_n \cos(k_n \alpha - \omega_n t + \epsilon_n) > 1 \tag{34}$$

must therefore be investigated.

The three moments given by

$$\psi_o = \int_o^\infty S(k)\, dk \tag{35}$$

$$\psi_1 = \int_o^\infty S(k)\, k\, dk \tag{36}$$

and

$$\psi_2 = \int_o^\infty S(k)\, k^2\, dk \tag{37}$$

need to be considered in this connection, and from (34) it is evident that ψ_2 must exist and be bounded.

The probability that m will be less than zero is given by

$$(38) \qquad p(m<0) = \frac{1}{\sqrt{2\pi\psi_2}} \int_1^\infty e^{-t^2/2\psi_2}\, dt = \frac{1}{\sqrt{2\pi}} \int_{1/\sqrt{\psi_2}}^\infty e^{-t^2/2\psi_2}\, dt .$$

Equation (38) may be interpreted to be the probability that some particle, α_o, will be found at the top of a loop between the points where $z = z(x)$ is vertical for some particular time of observation. Such a particle is surely involved in a breaking wave. Other particles that do not satisfy this condition also may be involved in a breaker.

Since the spectrum $S(k)$ has not as yet been measured, it is necessary to investigate possible relationships between $S(k)$ and spectra of $z(x, 0)$ and $z(0, t)$ before estimating the probability in (38).

Marginal distribution of $z=z(x)$

The graphical construction used to illustrate the generation of the random function $z = z(x)$ can be used to obtain the marginal distribution of $z = z(x)$. The joint density of $z(\alpha, 0)$ and $\frac{dx}{d\alpha} = m(\alpha, 0)$ is bivariate normal. The variance of $z(\alpha)$ is ψ_o, the variance of $m(x)$ is ψ_2, and the covariance is $-\psi_1$ as defined in (34), (35) and (36).

If $f(z, m)$ is the bivariate normal distribution of z and m, we note that

$$(39) \qquad F(z,m) = f(z,m)m$$

nearly has the required properties of a probability density function since m is dimensionless and $E(m) = 1$. Also since x and α have the same dimensions, a given number of equally spaced points in a small interval of a given length over α produce m times this number of points with this same spacing in an interval of a different size on the x axis.

The function $F(z, m)$ is not a probability density function strictly because it is negative for $m < 0$, but this corresponds physically to impossible configurations of $z = z(x)$, and points on $z = z(x)$ generated when $m < 0$ will be shown to have extremely low probabilities. Actually even more points on $z = z(x)$ are probably destroyed by the breaking process, and $z = z(x)$ is modified in form long before m becomes zero for some sea conditions.

However, as an approximation, we can truncate $F(z, m)$ at $m = 0$ and renormalize. Thus

(40) $$\int_{-\infty}^{\infty}\left[\int_{o}^{\infty}F(z,m)dm\right]dz = \frac{1}{\sqrt{2\pi}}\left[\int_{-1/\sqrt{\psi_2}}^{\infty}e^{-\xi^2/2}\,d\xi + \sqrt{\psi_2}\,e^{-1/2\psi_2}\right] = K$$

Then

(41) $$E(z) = \frac{1}{K}\int_{-\infty}^{\infty}\left[\int_{o}^{\infty}z\,F(z,m)dm\right]dz = -\frac{\psi_1}{K\sqrt{2\pi}}\left[\int_{1/\sqrt{\psi_2}}^{\infty}e^{-\xi^2/2}\right]$$

(42) $$E(z^2) = \frac{\psi_o}{K\sqrt{2\pi}}\left[\int_{-1/\sqrt{\psi_2}}^{\infty}e^{-\xi^2/2}\,d\xi + \left(1+\frac{\psi_1^2}{\psi_o\psi_2}\right)\sqrt{\psi_2}\,e^{-1/2\psi_2}\right]$$

(43) $$E(z^3) = \frac{-\psi_1}{\sqrt{2\pi}\,k}\left[3\psi_o\int_{-1/\sqrt{\psi_o}}^{\infty}e^{-\xi^2/2}\,d\xi - \frac{\psi_1^2}{\psi_2^{3/2}}e^{-1/2\psi_2}\right]$$

Also the probability density function is given by

(44) $$p(z)=\frac{e^{-\frac{1}{2}\frac{z^2}{\psi_o}}}{K2\pi\sqrt{\psi_o}}\left[\left(1-\frac{\psi_1}{\psi_o}z\right)\int_{-\frac{(1-\psi_1 z/\psi_o)\sqrt{\psi_o}}{\sqrt{\psi_o\psi_2-\psi_1^2}}}^{\infty}e^{-\xi^2/2}d\xi + \frac{\sqrt{\psi_o\psi_2-\psi_1^2}}{\psi_o^{\frac{1}{2}}}e^{-[(1-\psi_1 z/\psi_o)^2\psi_o/\psi_o\psi_2-\psi_1^2]/2}\right]$$

If ψ_2 is small compared to one,

(45) $$E(z) = -\psi_1$$

(46) $$E(z^2) = \psi_o$$

(47) $$E(z^3) = 3\psi_1\psi_o$$

and

(48) $$p(z) = \frac{e^{-z^2/2\psi_o}}{\sqrt{2\pi}\,\psi_o^{\frac{1}{2}}}\left(1-\frac{\psi_1}{\psi_2}z\right)$$

Let

(49) $$z' = z + \psi_1 .$$

Then

(50) $$p(z') = \frac{e^{-(z'-\psi_1)^2/2\psi_o}}{\sqrt{2\pi}\,\psi_o}\left(1+\frac{\psi_1^2}{\psi_o}-\frac{\psi_1 z'}{\psi_o}\right)$$

and

(51) $$E(z') = 0$$

(52) $$E(z'^2) = \psi_o - \psi_1^2$$

(53) $$E(z'^3) = 0$$

(54) $$E(z'^4) = 3\psi_o^2 - 6\psi_o\psi_1^2 - 3\psi_1^4$$

The skewness is zero and the coefficient of excess is $-6\psi_1^4 / (\psi_o - \psi_1^2)^2$.

Estimates of ψ_o, ψ_1, and ψ_2

From (52) the average of $z'(x)$ is zero and the variance is, say, $\psi_o{}^* = \psi_o - \psi_1^2$. This is the variance that is estimated by a free surface wave record.

Since

(55) $$S(k)\,dk = S(\frac{\omega^2}{g})\,\frac{2\omega\,d\omega}{g} = S'(\omega)\,d\omega$$

$$= S''(f)\,df \quad ,$$

and since (for example)

(56) $$S(k)\,k^2\,dk = S''(f)\,16\pi^4\,\frac{f^4}{g^2}\,df$$

let us assume that

(57) $$S''(f) = \begin{cases} K/f^n & f_\ell < f < f_u \\ 0 & \text{otherwise} \end{cases}$$

From equations (35), (36), (37), (55), (56), and (57), one can obtain the result that

(58) $$\psi_o = \psi_o{}^*\left(\frac{2}{1+D}\right)$$

(59) $$\psi_1 = \frac{4\pi^2}{g}\left(\frac{n-1}{n-3}\right)\psi_o{}^*\left[\frac{1-(f_\ell/f_u)^{n-3}}{1-(f_\ell/f_u)^{n-1}}\right]\left(\frac{2}{1+D}\right)f_\ell^2$$

and

(60) $$\psi_2 = \frac{16\pi^4}{g^2}\left(\frac{n-1}{n-5}\right)\psi_o{}^{*}\left[\frac{1-(f_\ell/f_u)^{n-5}}{1-(f_\ell/f_u)^{n-1}}\right]\left(\frac{2}{1+D}\right)f_\ell{}^4$$

where

(61) $$D = \left(1 - \frac{64\pi^4}{g^2}\left(\frac{n-1}{n-3}\right)^2\left[\frac{1-(f_\ell/f_u)^{n-3}}{1-(f_\ell/f_u)^{n-1}}\right]^2 f_\ell{}^4(\psi_o{}^{*})\right)^{\frac{1}{2}}.$$

For one fairly severe storm at sea ψ_o^{*} was about equal to 116 ft^2 and f_ℓ was equal to 0.046. The results above permit an investigation of the sensitivity of the particle motion moments to the values of n and f_u.

Tables 1 through 5 give the values of ψ_o, ψ_1, ψ_2, $1/\sqrt{\psi_2}$, and $\psi_1^2/\psi_o\psi_2$ for various values of n and for $f_u = 0.46$, 0.92, 4.6 and ∞. The values of f_u correspond to periods of 2.16, 1.08, .216 and zero seconds.

Table 1.

Values of ψ_o for various values of n and f_u for $\psi_o{}^{*} = 116$ ft^2 and $f_\ell = 0.046$ sec^{-1}.

n \ f_u	0.46	0.92	4.6	∞
5.9	116.26	116.26	116.26	116.26
5.7	116.28	116.28	116.28	116.28
5.5	116.30	116.30	116.30	116.30
5.3	116.32	116.32	116.32	116.32
5.1	116.35	116.35	116.35	116.35
4.9	116.38	116.39	116.39	116.39
4.7	116.42	116.43	116.44	116.44
4.5	116.47	116.49	116.50	116.50

Table 2.

Values of ψ_1 for various values of n and f_u for $\psi_o{}^* = 116\ \text{ft}^2$ and $f_\ell = 0.046\ \text{sec}^{-1}$.

n \ f_u	0.046	0.92	4.6	∞
5.9	0.51	0.51	0.51	0.51
5.7	0.53	0.53	0.53	0.53
5.5	0.55	0.55	0.55	0.55
5.3	0.57	0.57	0.57	0.57
5.1	0.59	0.59	0.59	0.59
4.9	0.62	0.62	0.62	0.62
4.7	0.65	0.66	0.66	0.66
4.5	0.69	0.70	0.71	0.71

Table 3

Values of ψ_2 for various values of n and f_u for $\psi_o{}^* = 116\ \text{ft}^2$ and $f_\ell = 0.046\ \text{sec}^{-1}$.

n \ f_u	0.46	0.92	4.6	∞
5.9	.0034	.0036	.0038	.0039
5.7	.0038	.0042	.0046	.0048
5.5	.0044	.0049	.0057	.0064
5.3	.0051	.0060	.0076	.0102
5.1	.0060	.0075	.0105	.0290
4.9	.0072	.0097	.0162	∞
4.7	.0087	.0127	.0261	∞
4.5	.0107	.0167	.0446	∞

Table 4.

Values of $1/\sqrt{\psi_2}$ for various values of n and f_u for $\psi_o{}^* = 116\ \mathrm{ft}^2$ and $f_\ell = 0.046\ \mathrm{sec}^{-1}$.

f_u n	0.46	0.92	4.6	∞
5.9	17.2	16.7	16.2	16.1
5.7	16.2	15.5	14.8	14.5
5.5	15.2	14.2	13.2	12.5
5.3	14.1	12.9	11.5	9.9
5.1	12.9	11.5	9.8	5.9
4.9	11.8	10.2	7.9	0
4.7	10.7	8.9	6.2	0
4.5	9.7	7.7	4.7	0

Table 5.

Values of $\psi_1{}^2/\psi_o\psi_2$ for various values of n and f_u for $\psi_o{}^* = 116\ \mathrm{ft}^2$ and $f_\ell = 0.046\ \mathrm{sec}^{-1}$.

f_u n	0.46	0.92	4.6	∞
5.9	0.67	0.63	0.60	0.59
5.7	0.63	0.58	0.53	0.51
5.5	0.59	0.52	0.45	0.40
5.3	0.54	0.46	0.37	0.27
5.1	0.50	0.40	0.29	0.10
4.9	0.46	0.34	0.21	0
4.7	0.42	0.29	0.14	0
4.5	0.38	0.25	0.10	0

Discussion of tables

The assumption that the range that has been assumed for the values of f_u and n for the spectral forms for $S(k)$ must first be questioned. The range of f_u is probably more than adequate. However, the relationship between particle motion spectra and free surface spectra is not known. Perhaps n can be even smaller than 4.5 and still yield spectra for the free surface that behave over a given range like $1/f^p$ where p is greater than 5 as wave observations seem to suggest.

If these assumed values are reasonable, it would follow that a loop in a realization, $z = z(x)$, would be a very rare event. The smallest value (except the zero) in Table 5 is 4.7 and the associated probability is less than 10^{-5}. If loops were identified with breaking waves, the results would imply that waves shorter than 0.2 feet and n's less than 5 produce such breakers and this does not seem at all reasonable.

Stated another way, results based on spectra like K/f^5 depend very strongly on the high frequency tail of the spectrum where the waves are less than 3 inches long and on the fact that the exponent is exactly 5 and not 5.1. The original conditions correspond to waves with a significant height of 42 feet and with representative lengths of 1500 to 2000 feet. Breakers in such a sea certainly occur and surely have dimensions exceeding 3 inches. Thus although such loops identify unrealistic spectra, the limitations on the spectral form appear to be due to effects that occur before such loops even have a chance to attempt to form.

The tables also suggest that equation (49) will be approximately correct as to general shape, and that the higher moments are both difficult to detect theoretically and to measure in practice. Equations (45), (46), and (52) are satisfactory approximations, but the approximate higher moments and skewness and kurtosis values will be in error by large percentages. The distribution of z as given by equation (44) when graphed for two conditions, one for which $f_u = 0.46$ and $n = 5.9$, the other for which $f_u = 4.6$ and $n = 4.5$ can hardly be distinguished visually from the normal curve.

Second order periodic breaker effects

The Gerstner wave satisfies the nonlinear Lagrangian equations exactly. However, a particle never moves far away from its mean position. A strong field of vorticity exists. The limiting steepness of a Gerstner wave is given by $ak = 1$. For irrotational waves Michell [1893) has shown that $\frac{2a}{\lambda} = 0.142$, and $ak = 1$ corresponds to $\frac{2a}{\lambda} = 0.32$ which yields a wave much steeper than is possible for irrotational motion. It was mentioned above that the Gerstner wave could be made irrotational to second order (with third order complications) by adding an appropriate drift current. With θ equal to zero, this drift current becomes $a^2\omega k$.

The parametric representation for the free surface then becomes

$$x = \alpha - a \sin(k\alpha - \omega t) + a^2 k \, \omega t$$
$$z = a \cos(k\alpha - \omega t) \qquad (62)$$

for a periodic wave, which can be transformed by solving for α in the second equation to become

$$\cos^{-1}(z/a) - ak \sin(\cos^{-1}(z/a)) = kx - \omega t - a^2k^2 \omega t \qquad (63)$$

and therefore the phase speed obtained from the Lagrangian equations solved for irrotational motion to second order becomes

$$C = \frac{g}{\omega}(1 + a^2k^2) \, . \qquad (64)$$

The phase speed obtained by solving the Eulerian equations to third order for irrotational motion is given by

$$C = \frac{g}{\omega}\left(1 + \frac{a^2k^2}{2}\right) \qquad (65)$$

The Lagrangian waves to second order are thus not consistent with Eulerian waves to third order. The second order periodic irrotational Gerstner waves appear to be traveling as if the linear phase speed had been simply added to the drift current. Third order periodic irrotational Eulerian waves have a drift current that is the same as the Gerstner wave, but the phase speed correction is only half of the phase speed correction for Gerstner waves. The discrepancy can be explained by noting

that there probably is a residual vorticity field at third order in the Lagrangian solution that may account for the difference.

The particle velocity at the crest for the Gerstner wave is

(66)
$$u(0,0) = \left.\frac{dx}{dt}\right/_{\alpha=0,t=0} = a\omega + a^2 k\omega \ ,$$

and when the phase speed is set equal to the particle velocity, the limiting form

(67)
$$ak = 1$$

is still obtained.

With $ak = 1$, the second order phase speed and the particle velocities at the crest are exactly double that of the linear theory, but it is known that the phase speed due to finite height cannot exceed about 1.2 times the linear phase speed. These results are all indicative of the need for different wave models and for measurements of higher order effects in waves.

Construction of $z = z(x)$ for the second order equations

From recent results of Tick [1961], it may be possible by starting with equations (28) to construct the vector process given below by an appropriate sequence of operations on the linear realizations constructed above.

$$\begin{gathered}
x(\alpha, 0, 0)\\
z(\alpha, 0, 0)\\
x(\alpha, \tau, 0)\\
z(\alpha, \tau, 0)\\
x(\alpha, 0, \delta_1)\\
z(\alpha, 0, \delta_1)\\
x(\alpha, \tau, \delta_1)\\
z(\alpha, \tau, \delta_1)\\
x_t(\alpha, 0, 0)\\
x_t(\alpha, 0, \delta_1)
\end{gathered}$$

The construction may even turn out to be considerably simpler than that employed by Tick [1961] because only low frequencies are involved.

In the above process, τ is to be a fraction of a second after $t = 0$, δ_1 is to be a foot or so below the free surface. The first two pairs will yield an estimate of the instantaneous speed of a crest. If $x_t(\alpha, 0, 0)$ exceeds this value, then the crest could be considered to be a breaking crest. The other terms should yield some information on the size of the region of unstable motion. A range of possible spectral forms can be used to construct this vector process and some idea of the fraction of breaking waves in the total can be gained.

However, from the results given above on the linear random model and on the periodic second order irrotational model, the results obtained from such a construction will probably not be quantitatively correct as they may yield waves that are too high physically by a factor of two, even for irrotational waves to second order.

Breakers in a random sea

Whitecaps and breakers in deep water are an integral part of the problem of wave generation. Many photographs of waves in deep water show such breaking waves. The equations governing the wave motion fail locally and a breaker is produced. The water in the breaking part of a wave is certainly governed by physical laws that are completely different from those that govern the wave motion. A breaker is probably produced when the water particle speed exceeds the speed of the crest, but other effects such as the wind actually blowing off the crest of a wave before this requirement is met may also play an important part.

Moreover, the turbulence produced by a breaking wave, governed by eddy viscosity laws, will tend to damp out the higher frequency linear components in the spectrum of the wind generated sea. The absence of the local chop in the wake of a ship illustrates this effect.

Whenever a breaker disorganizes the fluid motions, there is a mass of water moving forward at the crest of the waves. This effect may contribute to both the drift current at the surface and to the growth of the lower frequency waves.

Also there is a wind drift current in a local sea that is nearly in the same direction as the traveling waves. This wind drift current produces a field of vorticity in the same sense as the direction of propagation of the waves and may well cause breaking to occur for considerably lower wave heights than even irrotational theory would predict.

The work of Longuet-Higgins [1953], [1960] has shaken the concepts of irrotational motion for gravity waves to their very foundation . His results predict that, even in the absence of wind drift currents and turbulent effects due to breakers, the mass transport velocity in deep water may be considerably stronger than irrotational theory predicts if the waves have been running long enough.

Moreover, as Longuet-Higgins [1953] has pointed out, Duvriel-Jacotin has shown that any mass transport velocity can be used as the starting point and a wave motion can be superimposed thereon.

It is also known from classical periodic wave theory that a sharp angle at the crest of 120° is another way to define the limiting height of a periodic wave of the form $z = z(x)$. It may be possible if the other concepts discussed above fail, due to the fact that the results are only to second order, to study constructions of $z = z(x)$ as a random process to see how many waves approach this limiting form.

With all of these preliminary remarks it would seem that equation (29), with perhaps still an arbitrary second order vorticity field added, can provide some insight on the growth of a wave spectrum. Consider two orbital motion spectra with the same variance, one with contributions with relatively higher frequencies than the other. The mass transport at the surface will be stronger for the spectrum with the richer high frequency content but at the same time the speeds of the crests will be less. The interaction of these effects could conceivably cause the higher frequency waves in the spectrum as they are overtaken by and ride up on the crests of the longer lower frequency waves (Longuet-Higgins and Stewart [1960]) to break and dissipate by turbulent action. At the same time the low frequency components can continue to grow and even be caused to grow by the breaking of the shorter waves. Considerations such as this may explain various wave spectra where forms like K/ω^7, K/ω^6, $K/\omega^{5.5}$, and K/ω^5 have been proposed and where the exponent

appears to depend on the heights of the waves that were measured.

Comparison with observations

The purpose of this part of this paper is to present the results of some observations that suggest that the various models proposed above are more nearly in accord with actual waves than models based on the Eulerian equations.

Figure 4 is a copy of a photograph given by Roll [1957] for waves a few centimeters high and 8 to 35 cm long. The third photograph from the top shows a remarkable similarity to figure 2. For various wave heights and apparent lengths, either a rounded crest or a sharp crest occurs. Note the marked departure from normality that slopes and curvatures would have if they were evaluated from such a record.

Figures 5, 6, and 7 show some reproductions of seven selected wave profiles obtained by stereo-photogrammetric techniques from photographs taken aboard a ship. The height scale is five times that of the horizontal scale. The profiles show the presence of sharp crests and shallow troughs as these models predict. Note also that the profiles are much richer in high wave numbers than corresponding time histories are rich in high frequencies. These profiles were kindly furnished the author by Dr. Norman F. Jasper of the David Taylor Model Basin. Additional information on these records is given by Brooks and Jasper [1957].

Figure 8 shows some selected time histories obtained in Buzzards Bay by Harlow G. Farmer [Farmer and Ketchum (in press)]. The original records have been reversed, so that time increases from left to right, and blackened below the original trace. The wave sensing system consists of a very fine wire (0.015 inch diameter) that appears to follow the water elevation more accurately than previous wave poles or wave wires. A number of the crests are very sharply pointed. There is evidence that a breaker occurred in the top trace where one crest shows a nearly vertical rise at the crest. Since these records are much richer in high frequency content (sharp crests, and vertical rises), spectra computed from them will be richer at high frequencies than spectra previously reported for waves in this general range of heights and periods.

The figures and illustrations in Schulejkin [1960] also suggest that the randomized Lagrangian model corresponds well with reality.

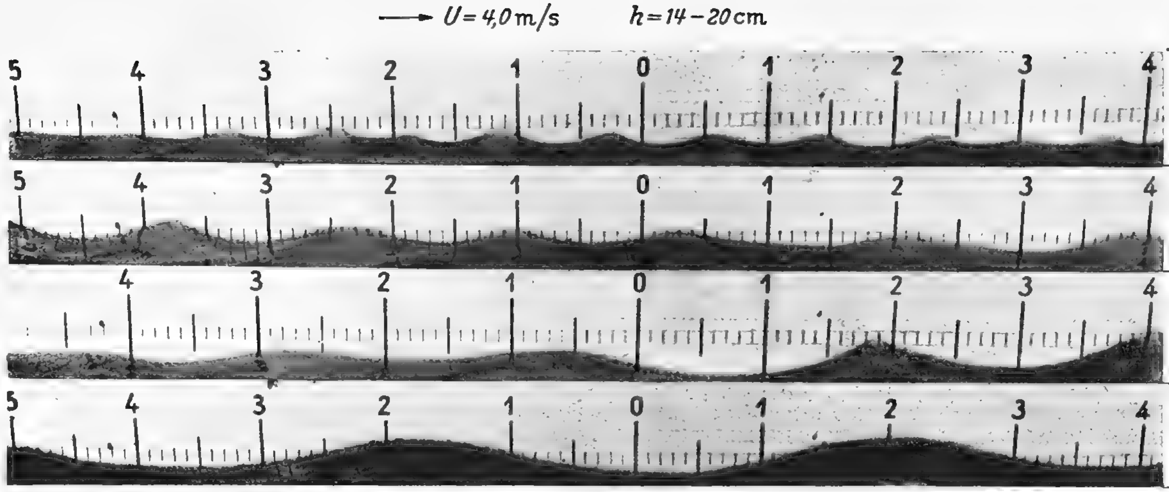

F m	$\overset{\approx}{H}$ cm	$\overset{\approx}{L}$ cm	$\overline{H/L}$
5 – 6	0,9	7,8	1 : 9
9 – 10	1,5	15,0	1 : 10
15 – 16	2,0	21,2	1 : 11
35 – 36	2,8	35,5	1 : 13

Figure 4. Photographs of waves after Roll [1957].

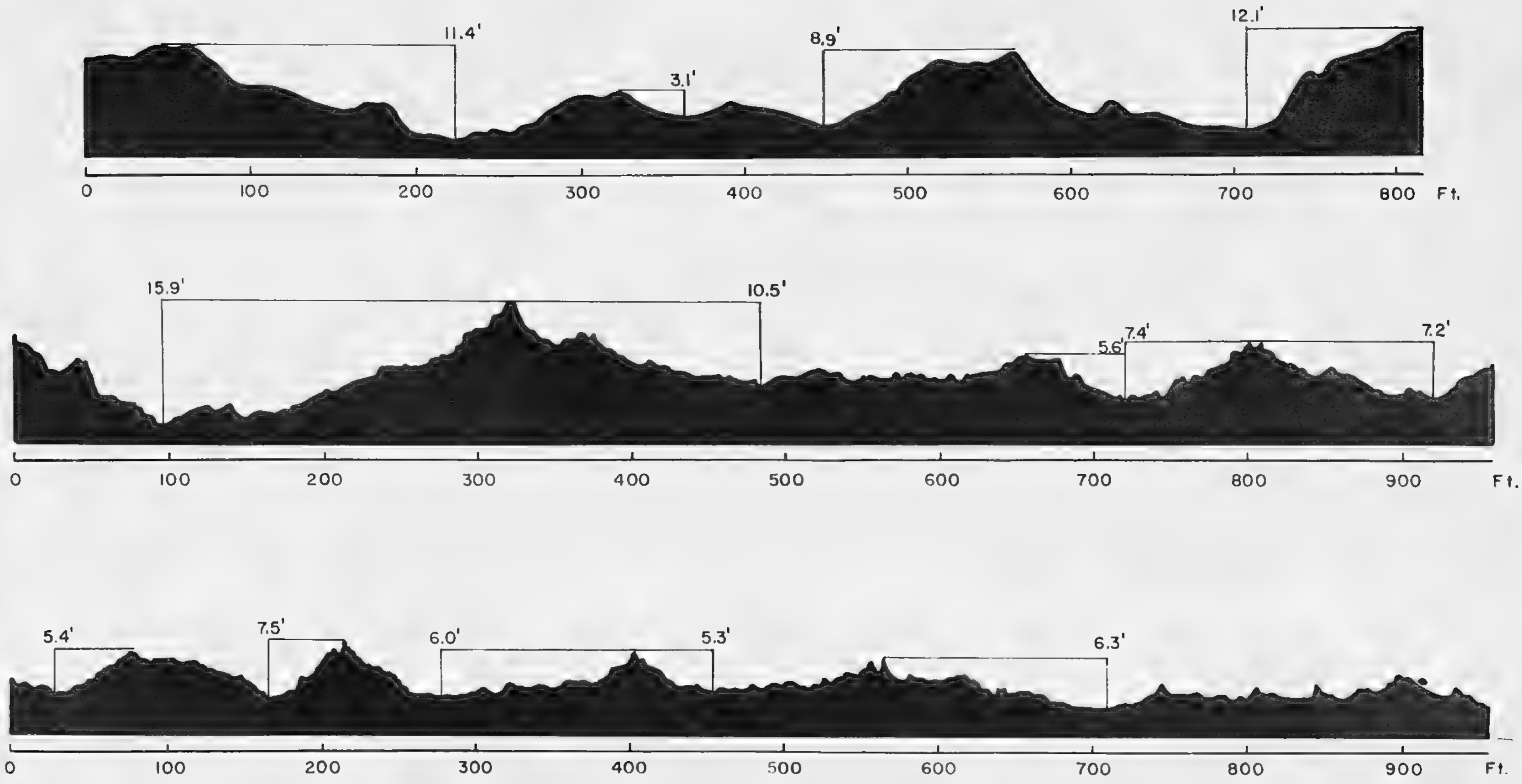

Fig. 5. Selected wave profiles obtained by stereophotogrammetric methods.

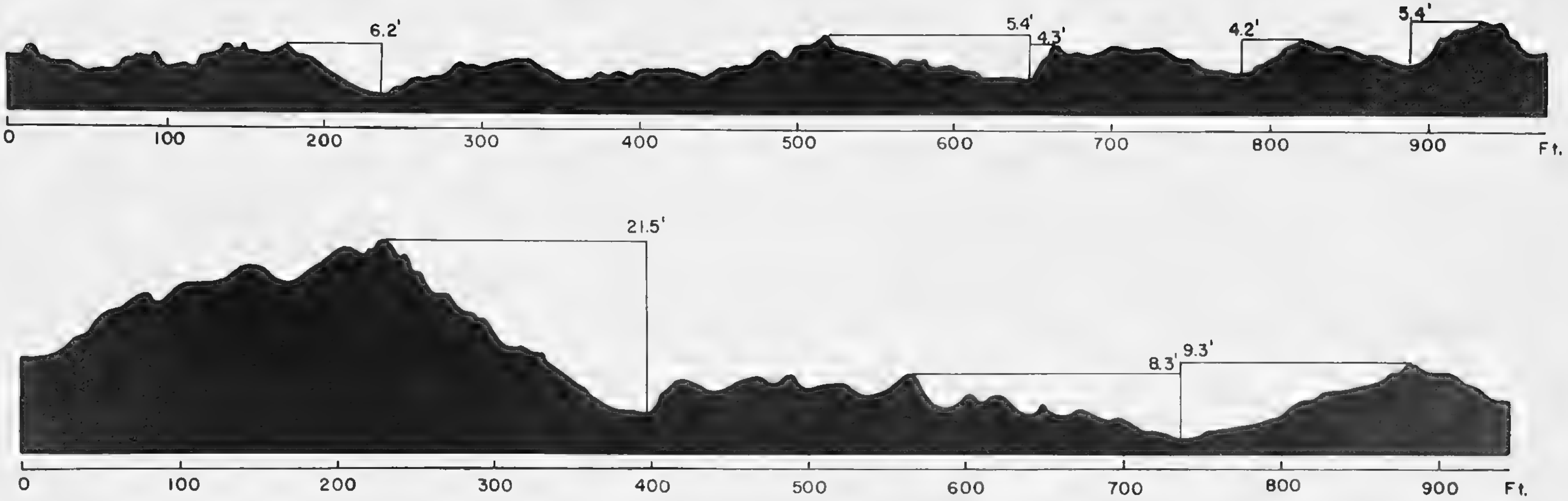

Fig. 6. Selected wave profiles obtained by stereophotogrammetric methods.

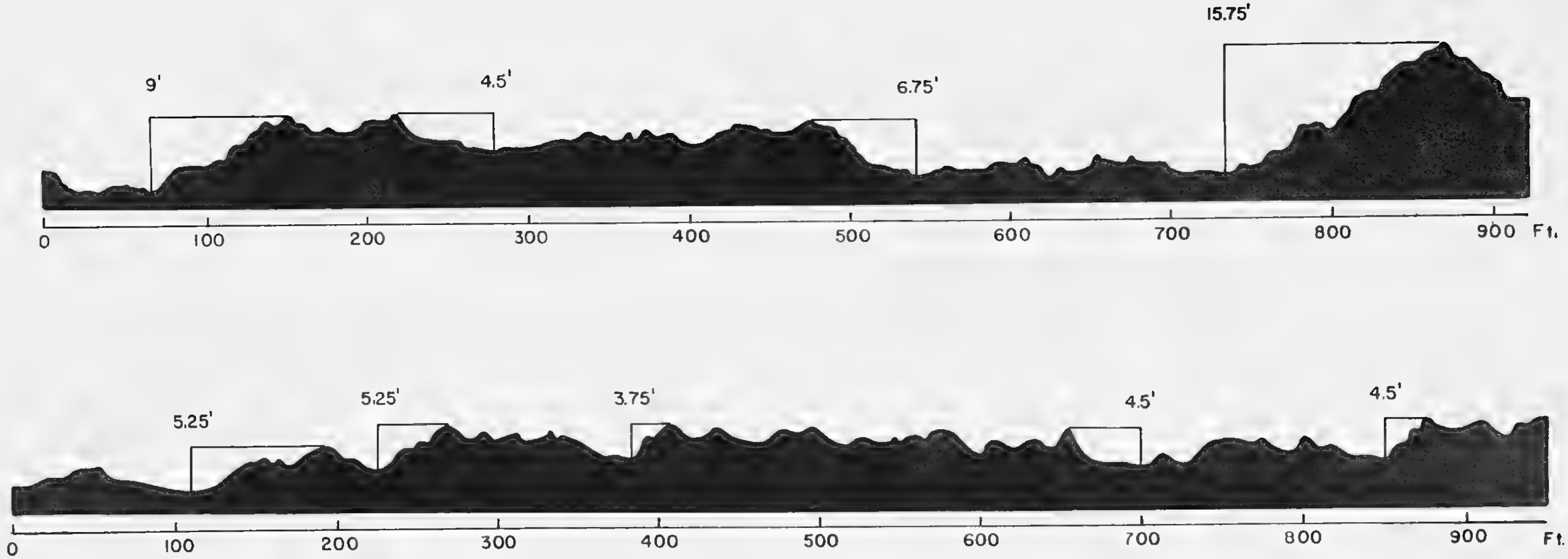

Fig. 7. Selected wave profiles obtained by stereophotogrammetric methods.

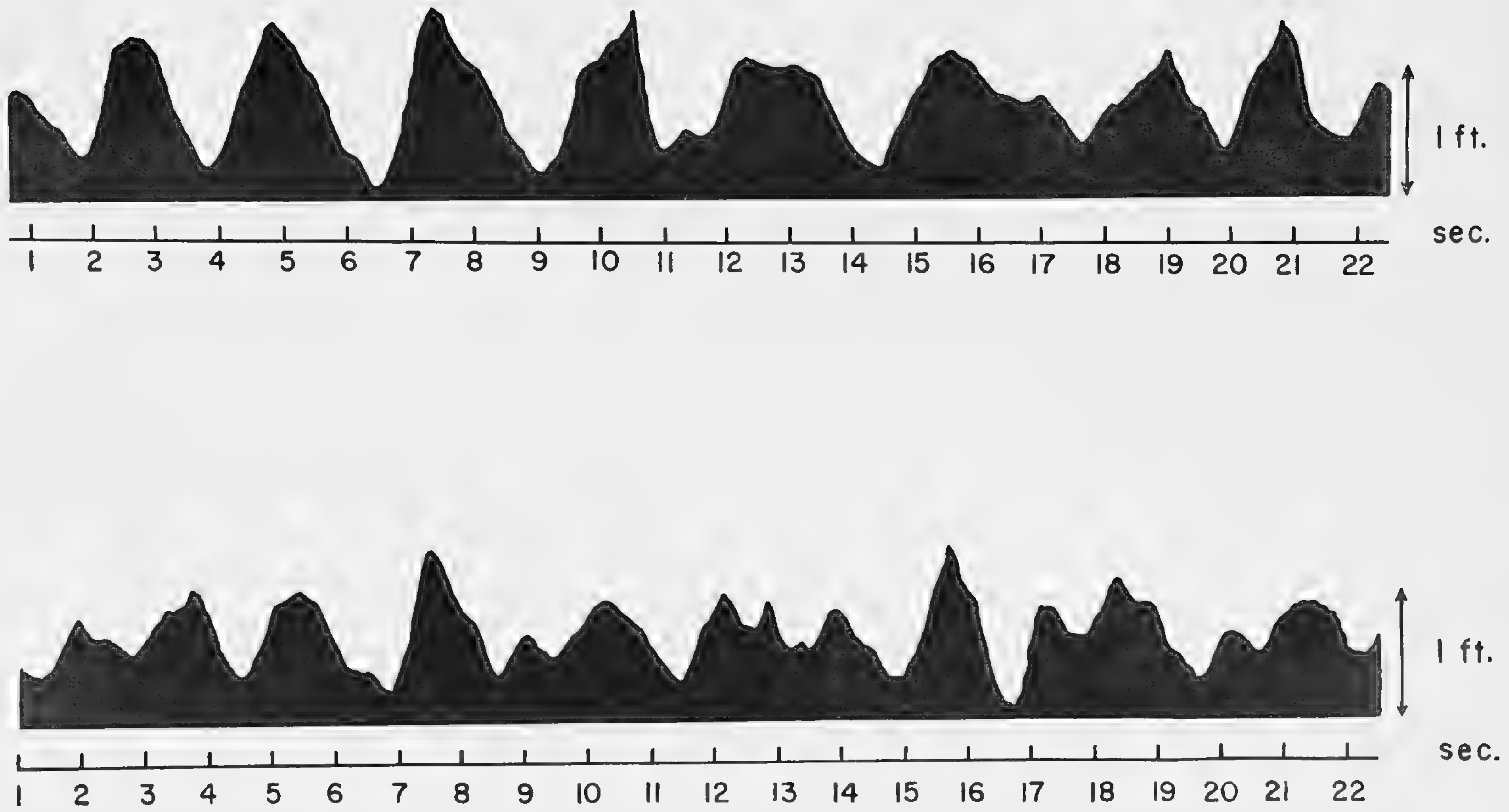

Fig. 8. Time histories of waves obtained in Buzzards Bay.

Summary

The three models based on the Lagrangian equations proposed in this paper show some features of waves that are observed to occur and that do not appear to be present in models based on the Eulerian equations. The probability structures of the various resulting free surfaces are not understood. However, in the simplest model, free surfaces can be constructed that show very interesting properties. There is some hope that the effects of breaking waves can be studied by means of these models. It is also evident that the measurement of random seas needs to be considerably refined so as to detect the higher order effects possible in these various different models.

Acknowledgments

The material presented in this technical report was stimulated by a conversation with Dr. Leo J. Tick in which he asked whether or not random wave theory could be approached from any other point of view than that presently in use. If breaking waves are ever to be studied at all, the perturbation procedure in the Eulerian system of equations does not seem to come close enough soon enough. These results are a start toward trying to understand waves from another point of view. The help of Dr. Tick in the formulation of the theoretical developments is also appreciated.

Stimulating conversations with Dr. G. Neumann with reference to eddy viscosity effects and visual nonlinear effects of breakers were most helpful.

References

Biesel, F. [1952]: Study of wave propagation in water of gradually varying depth. In Gravity Waves. Natl. Bur. Standards (U.S.) Circ. 521, pp. 221-234.

Brooks, R. L., and N. F. Jasper [1957]: Statistics on wave heights and periods for the North Atlantic Ocean. DATMOBAS Report 1091.

Cartwright, D. E., and L. J. Rydill [1956]: The rolling and pitching of a ship at sea. Trans. I. N. A. (London), vol. 98, p. 100.

Ehrenfeld, Goodman, et al. [1958]: Theoretical and observed results for the zero and ordinate crossing problems of stationary Gaussian noise with application to pressure records of ocean waves. Tech. Report No. 1, Bureau of Ships, Contract No. Nobs 27018 (1734F), New York University, College of Engineering, Research Division.

Farmer, H. G., and D. D. Ketchum [in press]: An instrumentation system for wave measurements, recording and analysis. Proc. 7th Conference on Coastal Engineering.

Lamb, H. [1932]: Hydrodynamics, 6th Ed. Cambridge Univ. Press.

Lewis, E. V. [1955]: Ship speeds in irregular seas. Trans. SNAME, vol. 63.

Longuet-Higgins, M. S. [1953]: Mass transport in water waves. Phil. Trans. Roy. Soc. of London, Series A, vol. 245, pp. 535-581.

Longuet-Higgins, M. S. [1957]: Statistical properties of a random moving surface. Phil. Trans. Roy. Soc. of London, Series A, vol. 250, pp. 157-174.

Longuet-Higgins, M. S. [1960]: Mass transport in the boundary layer at a free oscillating surface. J. Fluid Mechanics, 8, 293-306.

Longuet-Higgins, M. S., and R. W. Stewart [1960]: Changes in the form of short gravity waves on long waves and tidal currents. J. Fluid Mech., 8, 565-583.

Michell, J. H. [1893]: The highest wave in water. Phil. Mag., 36, 430-437.

Phillips, O. M. [1958]: The equilibrium range in the spectra of wind-generated waves. J. Fluid Mechanics, vol. 4, part 4, pp. 426-434.

Phillips, O. M. [1961]: The dynamics of random finite amplitude gravity waves (preprint). NAS-NRC Conference on Ocean Wave Spectra, May 1-4, 1961.

Pierson, W. J. [1952]: A unified mathematical theory for the analysis, propagation and refraction of storm generated ocean surface waves. Parts I and II. Research Division, College of Engineering, New York University. Prepared for the Beach Erosion Board, Department of the Army, and Office of Naval Research, Department of the Navy.

Pierson, W. J. [1955]: Wind Generated Gravity Waves. Advances in Geophysics, vol. 2, Academic Press.

Pierson, W. J., and P. Fife [1961]: Some nonlinear properties of long crested periodic waves with lengths near 2.44 centimeters. Journal of Geophysical Research, vol. 66, no. 1.

Roll, H. U. [1957]: Oberflächen-Wellen des Meeres. Handbuch der Physik, (48), Berlin, Springer Verlag.

Schulejkin, W. W. [1960]: Theorie der Meereswellen. Akad. Verlag-Berlin.

St. Denis, M., and W. J. Pierson, Jr. [1953]: On the motions of ships in confused seas. Trans. Society of Naval Architects and Marine Engineers, vol. 61, pp. 280-357.

Stoker, J. J. [1957]: Water Waves. Interscience Publishers, New York.

Tick, L. J. [1959]: A nonlinear random model of gravity waves, I. Jour. Math. and Mech., vol. 8, no. 5.

Tick, L. J. [1961]: Non-linear probability models of ocean waves (preprint). NAS NRC Conference on Ocean Wave Spectra, May 1-4, 1961.